Chemical Engineering Science 278 (2023) 118888

Contents lists available at ScienceDirect

Chemical Engineering Science

journal homepage: www.elsevier.com/locate/ces

Design, techno-economic evaluation, and optimisation of renewable methanol plant model: Finland case study

Samuel Emebu [a,e,*], Clara Mendoza Martinez [b], Osaze Omoregbe [c,e], Aleksi Mankonen [b], Ebuka A. Ogbuoji [f], Ibrahim Shaikh [a], Even Pettersen [d], Marek Kubalčík [a], Charity Okieimen [e]

[a] Department of Automatic Control and Informatics, Faculty of Applied Informatics, Tomas Bata University in Zlín, Nad Stráněmi 4511, 760 05 Zlín, Czech Republic
[b] Department of Energy, Lappeenranta-Lahti University of Technology LUT, Yliopistonkatu 34, FI-53850 Lappeenranta, Finland
[c] Centre for Fuel Cell and Hydrogen Research, School of Chemical Engineering, University of Birmingham, Edgbaston, B15 2TT Birmingham, United Kingdom
[d] Department of Chemical Engineering, Norwegian University of Science and Technology, Høgskoleringen 1, 7491 Trondheim, Norway
[e] Department of Chemical Engineering, Faculty of Engineering, University of Benin, PO Box 1154, Benin City, Nigeria
[f] Department of Chemical and Materials Engineering, University of Kentucky, Lexington, KY 40506, USA

ARTICLE INFO

Keywords:
Central composite design (CCD)
Optimisation
Manufacturing unit cost
Conversion of carbon dioxide
Langmuir-Hinshelwood-Hougen-Watson (LHHW)
Cost-to-size model

ABSTRACT

The current global energy crisis, emphasises the need to simultaneously reduce fossil energy consumption, accelerate renewable energy development, and mitigate global warming, which may arise from situations of dirtier fuel usage. Consequently, this work highlights how captured carbon dioxide from fossil power and manufacturing plants, together with hydrogen purportedly produced via water electrolysis (powered by residual energy from fossil and renewable power plants), can be used to synthesize methanol. Therefore, a methanol plant model was proposed and designed. Multivariable regressions for the plant model were developed and optimised. Furthermore, deduced optimal were used to develop a Langmuir-Hinshelwood-Hougen-Watson (LHHW) kinetic equivalent to the Gibbs reaction model used in the simulation. Also, the plant cost analysis was performed at the optimal, and hydrogen cost was found to constitute the highest manufacturing cost component, hence the cost-determining factor of the plant. Finally, cost-to-size models for various cost components were also deduced.

1. Introduction

According to the European Commission's communication on energy prices, the global energy crisis of 2022, which is expected to spill over into 2023 (Taylor, 2022; Celasun et al., 2022), has necessitated a need to simultaneously reduce fossil energy consumption, and accelerate the development of renewable energy, as a supplementary energy source (Gielen and Bazilian, 2021). Renewable energy can improve energy security, mitigate global warming, and pollution (Gielen and Bazilian, 2021; European Environment Agency. Share of energy consumption from renewable sources in Europe, 2022; Albuquerque et al., 2020; Emebu et al., 2022). However, existing renewable energy technologies are currently unable to meet the energy demands resulting from the shortage of fossil fuel supply. Consequently, some countries have resorted to recommissioning older, dirtier coal-fuelled power plants (Ians, 2022; Frost, 2022). This situation exacerbates pollution caused by manufacturing plants and leads to further environmental concerns (Hunt et al., 2010). Therefore, to mitigate these environmental issues, it is necessary to incorporate carbon sequestration systems into such plants. Furthermore, by using carbon sequestration, and transforming hydrogen gas produced from electrolysis of water (powered by windmills, solar farms, tidal waves, or excess energy generated from fossil power plants during trough hours) into an effective energy medium, an alternative energy resource could be established through hydrogenation of captured carbon monoxide and dioxide into methanol (Nguyen and Zondervan, 2019) (Fig. 1).

Methanol, a liquid fuel with controlled flammability, easy transportation, storage, versatility, retrofitting capabilities, and the ability to serve as a fuel additive, offers advantages over hydrogen, despite hydrogen having the highest energy density (129–142 $kJ.g^{-1}$) (Vamvuka, 2011; Møller et al., 2017; Andersson and Grönkvist, 2019; Kandasamy et al., 2021:). Methanol also serves as a solvent and as a C_1 building block for producing other hydrocarbons such as acetic acid, methyl acetates, and formaldehyde (Bozzano and Manenti, 2016; Dalena et al., 2018:).

This work proposes the incorporation of a methanol production plant

* Corresponding author.
E-mail address: emebu@utb.cz (S. Emebu).

https://doi.org/10.1016/j.ces.2023.118888
Received 19 January 2023; Received in revised form 3 April 2023; Accepted 15 May 2023
Available online 19 May 2023

with power stations and other manufacturing plants, such as cement and pulp-and-paper mills, to reduce carbon dioxide emissions and store excess energy generated from power plants. Although renewable methanol production is reported to be less cost-effective than conventional methanol (Borisut and Nuchitprasittichai, 2019), due to plant investment cost, operating cost, and the cost of hydrogen gas (Holm-Larsen, 2001). The cost of hydrogen gas is variable and depends mainly on electricity cost, as well as current demand (Ball and Weeda, 2016; Zang et al., 2021; Schorn et al., 2021; Borisut and Nuchitprasittichai,). Therefore, it is reasonable to incorporate an inbuilt water electrolysis unit for hydrogen production (powered by residual energy from fossil or renewable power plants) into the methanol plant to reduce costs. Different methods of water electrolysis, such as alkaline, proton exchange membrane, and solid oxide electrolysis can be applied (Bos et al., 2020). While the effect of plant investment cost is primarily determined by the size or production rate of the plant, which is evaluated at the beginning of the plant installation and is considered a fixed cost (Stokes and Stokes, 2002; Nyári, 2018). On the other hand, the effect of operating cost on methanol production cost depends on the operating conditions such as temperature, and pressure under which the plant is designed (Borisut and Nuchitprasittichai, 2020; Moioli and Schildhauer, 2022). Therefore, to enhance the cost-effectiveness of the plant operations, it is essential to develop and optimise a well-designed plant model. Additionally, since an industrially sized methanol plant cannot be evaluated in the laboratory, commercial simulation software is necessary to achieve this objective.

Literature reports indicate that commercial chemical engineering software such as Aspen Hysys and Aspen Plus can be used for the modelling and simulation of methanol production plants (Borisut and Nuchitprasittichai, 2019; Borisut and Nuchitprasittichai, ; Borisut and Nuchitprasittichai, 2020; Aimiuwu et al., 2022; Van-Dal and Bouallou, 2013; Jeong et al., 2022). However, previous studies have not considered the effect of plant sizes in collaboration with reaction temperature and pressure on the optimisation of manufacturing costs, similar to **Noriega & Narvaez**'s report (Noriega and Narváez, 2020) on biodiesel plants. **Van-Dal & Bouallou** (Van-Dal and Bouallou, 2013) focused on modelling the reaction unit (specifically the Langmuir-Hinshelwood-Hougen-Watson, LHHW kinetic model) of a fixed-sized plant model, without considering plant economics. **Aimiuwu et al.** (Aimiuwu et al., 2022) simulated a fixed-sized plant model with variations of reaction conditions to highlight their effects on methanol conversion, selectivity, and yield. **Borisut & Nuchitprasittichai** (Borisut and Nuchitprasittichai, 2019; Borisut and Nuchitprasittichai, 2020) investigated the optimal reaction temperatures and pressure that minimises the manufacturing cost of a fixed-sized plant model. However, this approach did not consider the effect of plant size on the manufacturing cost. Considering the effect of plant sizes in collaboration with reaction temperature and pressure would help determine the limit at which it is necessary to expand the plant size beyond which there wouldn't be a significant reduction in manufacturing cost, since a larger plant results in lesser manufacturing cost (Holm-Larsen, 2001).

This paper aims to address the gaps identified in previous studies by focusing on optimising the plant size, reaction temperature, and pressure for a designed methanol plant model. Additionally, the determination of the exponential value of the cost-to-size model highlighted by **Remer & Chai** (Remer and Chai, 1993) at the estimated optimal conditions will be considered. The objectives of this study shall include: design and simulation of a methanol plant model with an integrated recycling system, heat integration, and wastewater discharge unit to meet European guidelines, using Finland as a case study; develop a Design of Experiment (DOE) of a three-factor (i.e., plant size, reaction pressure and temperature) inscribed Central Composite Design (CCD), with manufacturing cost, conversion of carbon dioxide, etc. as responses or objectives; size and cost estimation of unit operations, i.e., bare module, grassroots cost, manufacturing cost, etc., using the Capital Equipment Costing Program (CAPCOST) approach updated to today's value via the Chemical Engineering Plant Cost Index (CEPCI); calculate the manufacturing cost, conversion of carbon dioxide, amount of reactants and products from the methanol reactor, and other relevant data; develop statistically significant models (based on a p-value < 0.05) with the CCD in collaboration with calculated responses; Optimise the developed models with the necessary constraints to deduce optimal plant size, reaction temperature and pressure; elaborate the cost details

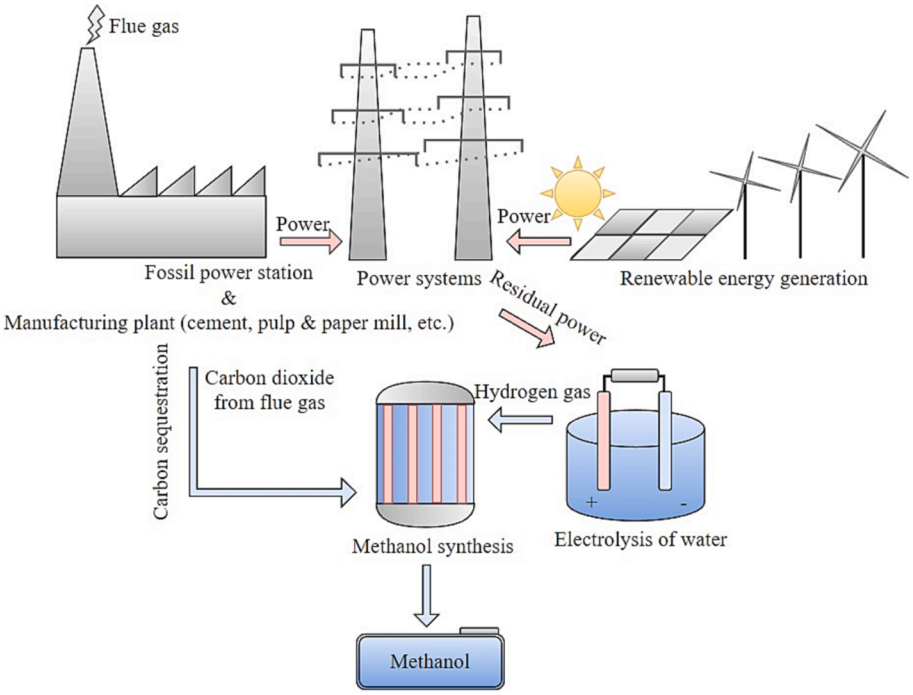

Fig. 1. Transformation of industrially captured carbon into methanol through hydrogenation.

of various unit operations at optimal conditions; and utilise the optimal conditions to deduce the exponential value of the cost-to-size model for the methanol plant.

2. Thermodynamics of methanol formation

The hydrogenation of carbon dioxide to methanol, represented by Equation (1), is an exothermic reaction that is more favourable at low temperatures and high pressures. However, due to the inert nature of carbon dioxide (Kanuri et al., 2022) and/or its tendency to form methane (its most stable reaction thermodynamics path (Etim et al., 2020)), initiating the reaction can be challenging. Therefore, suitable catalysts and reaction conditions are required to favour the methanol pathway (Etim et al., 2020; Porosoff et al., 2016). Additionally, the methanol pathway simultaneously triggers the Reverse Water Gas Shift (RWGS) reaction, represented by Equation (2), which produces carbon monoxide and water as by-products. The RWGS reaction is an endothermic hydrogenation of carbon dioxide at high temperature and low pressure, and its products reduce methanol selectivity (Zhong et al., 2020). Moreover, carbon monoxide can undergo exothermic hydrogenation to form methanol, as shown in Equation (3). The opposing temperature and pressure limits of these reactions mean that the average equilibrium shift, determined by the specific catalyst used, controls the product selectivity (Etim et al., 2020).

$$CO_2 + 3H_2 \leftrightarrow CH_3OH + H_2 \quad \Delta H^o = -49.16\,KJ.mol^{-1} \tag{1}$$

$$CO_2 + H_2 \leftrightarrow CO + H_2O \quad \Delta H^o = +41.21\,KJ.mol^{-1} \tag{2}$$

$$CO + 2H_2 \leftrightarrow CH_3OH \quad \Delta H^o = -90.77\,KJ.mol^{-1} \tag{3}$$

To speed up the methanol synthesis reaction, a temperature of at least 200 °C is required (Kanuri et al., 2022; Saeidi et al., 2014; Klerk, 2020:; Dimian et al., 2019). However, at high temperatures, the formulation of higher alcohols and hydrocarbons is observed, which can be suppressed in the presence of high amounts of carbon dioxide and at high pressures, ranging from 35 to 100 atm (Kanuri et al., 2022; Klerk, 2020:; Dimian et al., 2019; Din et al., 2019), or even as high as 148 atm (Yusuf and Almomani, 2023), in the presence of a suitable catalyst.

$$S = H_2/(2CO + 3CO_2) \geq 1.0 \tag{4}$$

Apart from economic considerations, the specific operating conditions of pressure, temperature, and hydrogen-to-carbon mole ratio, as represented by Equation (4) (Moioli and Schildhauer, 2022), are usually influenced by the activity of the catalyst used (Etim et al., 2020; Sarp et al., 2021). Generally, the catalysts are composites commonly made of copper, zinc, zinc oxide, aluminium oxide, zirconium, zirconium oxide, and other materials (Liu et al., 2003; Guil-López et al.,). Most catalysts used for methanol synthesis are copper-based materials because they are cheaper, and more efficient (Kamsuwan et al., 2021). One of the popular catalysts used in industrial methanol synthesis is the $Cu/ZnO/Al_2O_3$ catalyst (Zhang et al., 2022). The efficiency of methanol synthesis is largely dependent on the type of catalyst used in combination with its optimal temperature and pressure. **Sarp et al.** (Sarp et al., 2021) highlighted the performance of various catalysts, including their corresponding temperature, pressure, methanol yield, and hydrogen-to-carbon mole ratio. Specifically, it has been reported that $Cu/ZnO/Al_2O_3$ can catalyse industrial methanol production at 200–320 °C and 35–100 atm (Guil-López et al., 2020; Behrens, 2016; Jin et al., 2014). **Saito et al.** (Saito et al., 1995) reported a methanol yield of 0.721 $kg.hr^{-1}$ per kg of $Cu/ZnO/Al_2O_3$ at 225 °C, 49.3 atm, and a hydrogen gas to carbon dioxide ratio of 3. This yield is within the range reported by **Bukhtiyarova et al.** (Bukhtiyarova et al., 2017) for the space–time yield of commercial $Cu/ZnO/Al_2O_3$ at 200–260 °C, 29.6 atm, and a hydrogen gas to carbon dioxide ratio of 3.5. Note that it is conventional to recycle unreacted carbon monoxide, carbon dioxide, and hydrogen gas.

3. Detailed process overview and techno-economic evaluation

3.1. Process description

In this work, Finland was used as a case study to investigate the designed methanol plant model, as shown in Fig. 2, under varying production rates (40–1500 $kt.yr^{-1}$), temperature (200–300 °C), and pressure (35–148 atm) using hypothetical industrial $Cu/ZnO/Al_2O_3$ catalyst. It is assumed the plant is situated near a river, power plant (both fossil and renewable), cement factories, and pulp-and-paper plants, all of which have a combustion process capable of producing at least twice the amount of required carbon dioxide (for future plant expansion). The hydrogen gas required is produced on demand from electrolysis of water, using renewable energy source, and/or residual power from convectional power plant. The total cost of raw materials includes the cost of electrolysis of water (via the alkaline and/ PEM electrolysis method (Pérez-Fortes et al., 2016)) and captured carbon dioxide. It is assumed, carbon dioxide is captured using post-combustion monoethanolamine solvent absorption, a commercially available technology with 80–90% efficiency (Kuparinen et al., 2019), and it can be easily applied to an existing power plant to capture up to 365 kg CO_2 per MWh with an efficiency of 46% the heating value of the combustion process (IEAGHG. CO2 capture at gas fired power plants., 2012; Wang and Song, 2020). Additional carbon dioxide can be captured from an existing kraft pulp mill, (report indicates that 99 $kg.h^{-1}$ CO_2 can be captured from a 1500 $kt.yr^{-1}$ air-dry pulp plant (Kuparinen et al., 2019)), and from a cement factory (report suggests that current technology can capture 75 $kt.yr^{-1}$ CO_2, with a future capacity of 0.4–2 Mt CO_2 being planned (Olabi et al., 2022)). The expected capacity of the hydrogen gas production unit would be based on industrial water electrolysis, which can produce up to 5 $t.h^{-1}$ hydrogen at a net system efficiency of up to 70–75% (Olabi et al., 2022). The captured carbon dioxide and produced hydrogen gas are fed into the process at 1 atm, respectively at 45 °C (Siqueira et al., 2017; Jung et al., 2013; Warudkar et al., 2013), and 70 °C (Maeda et al., 2016; Hourng et al., 2017). If carbon dioxide is stored or transported over long distances, its feed pressure may approach 48 atm and its temperature may go below 45 °C (Wang et al., 2019). However, to effectively evaluate the effect of pressure on the methanol plant economics, it makes sense to implement it from the base pressure at which the carbon dioxide and hydrogen gases are produced, as done by **Nieminen et al.** (Nieminen et al., 2019). The cooling water is assumed to be pumped from a nearby river at 1.2–16 atm with an annual average temperature of << 15 °C (Tanttu and Jokela, 2018; Saarinen et al., 2010). Although 15 °C cooling water would be used for this process to ensure adequate allowance for the possibility of natural cooling of recycled heated water that is below 90 °C in an artificial reservoir. Heat energy can be sold to the Finland district heating network at an average temperature of 90 °C and a return average temperature of 50 °C at about 16 atm (Komu et al., 2021; Eliseev, 2011). Wastewater discharged back into the river must be cooled to about 40 °C to meet European guidelines (Finnish Water Utilities Association, 2018). Temperature differences between cooling water and hot fluids on heat exchangers are expected to be 5 °C (Bakar et al., 2015). The fluid from the reactor is cooled and separated using high-pressure, as well as low-pressure flash drums in two stages, at 50 °C for the first stage with the same pressure as the reactor, followed by throttling to 1 atm in the second stage. The resulting liquid phase is then distilled to about 99% pure methanol at the preceding pressure.

Please note that, in addition to the compression, reaction, phase separation, and distillation units, the designed plant model also include the pumping, heat exchanger, heater, and water treatment units. The "HEATER" and "PMP-2" are variable equipment, that may or may not be included in the model, depending on the designed temperature and pressure considered. The "AXLRY" unit operation is a heater used for calculation purposes.

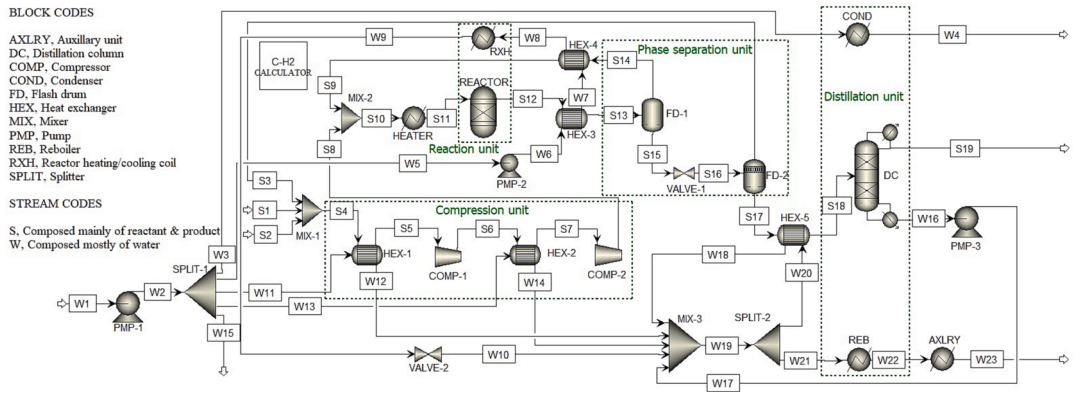

Fig. 2. Designed plant model for methanol production.

3.2. Process simulation, and thermodynamics

The methanol production process was simulated using Aspen Plus version 11.0 software. The reactor, compressors, distillation column, and reaction mixture stream through heat exchangers, as well as heaters were modelled using the Peng-Robinson property package (PENG-ROB). The steam table property package (Steam-TA) was applied to water streams in mixers, splitters, heat exchangers, and heaters. The Non-Random-Two-Liquid (NRTL) property package was used for throttling liquid in the separation unit to 1 atm. The thermodynamics of the PENG-ROB (Zohuri, 2018; Wang et al., ; Tosun, 2013) and NRTL (Vetere, 2004; Puentes et al., 2018; Kristensen et al., 1993) property packages are elaborated in literature.

In the simulation, the following predictive approach was used for unit operations. Heat exchangers were modelled using the GEN-HS model, specifying the hot or cold stream outlet temperature, with "shortcut" as the model fidelity. Compressors were modelled using the isentropic model with specifications of "discharge pressure" and "isentropic efficiency". A centrifugal pump with mechanical efficiency specification was used. The reactor was modelled using the RGibbs model, based on Gibbs free energy minimisation, with specifications for "calculation of phase equilibrium and chemical equilibrium" and two-phase calculation. The distillation column was modelled using the DSTWU model based on the Winn-Underwood-Gilliland shortcut method, with specifications for the number of stages, light, and heavy components.

3.3. Sizing of unit operation

To perform the economic evaluation of the methanol production process, adequate sizing of unit operations is required. Some unit operations, such as compressors, pumps, and heat exchangers are directly sized from the Aspen Plus simulation. The compressor, pump, and heater/cooler are sized based on the calculated power (kilowatts) required, while the heat exchanger, as well as distillation trays, are sized based on calculated areas (m^2). Other unit operations, such as the reactor, flash drum, distillation column, reboiler, and condenser, are sized based on their volume (m^3). Their volumes can be indirectly estimated from simulation results, together with the specifications highlighted in Table 1, as explained in Section (1.1) of the appendix.

3.4. Economic evaluation

The estimation of unit operations' capital cost through the module costing technique can be used to perform the economic evaluation of the methanol plant (Richard et al., 2018; West et al., 2008; Lemmens,). The plant module cost, C_{TM}, is calculated by adding up the individual bare module costs, C_{BM}, for all unit operations (n), according to Equation (5)–(8). To estimate the grassroots cost, C_{GR} for a new plant, the calculated value of C_{TM} is combined with the base bare module cost, C^{o}_{BM} (i.e., C_{BM} at atmospheric pressure and with carbon steel material), using Equation (6). The manufacturing cost, C_{OM}, as given by Equation (7) is determined by taking into account the grassroots, C_{GR}, operating labour, C_{OL}, utility, C_{UT}, raw materials, C_{RM}, wastewater treatment cost, C_{WT} and district heating savings, C_{DH}. It should be noted that C_{DH} represents the cost saved from feeding back hot water to the district heating network.

$$C_{TM} = \Sigma_{i=1}^{n} C_{TM} = 1.18\Sigma_{i=1}^{n} C_{BM} \quad (5)$$

$$C_{GR} = C_{TM} + 0.5\Sigma_{i=1}^{n} C^{o}_{BM} \quad (6)$$

$$C_{OM} = 0.18C_{GR} + 2.73C_{OL} + 1.23(C_{UT} + C_{RM} + C_{WT}) - C_{DH} \quad (7)$$

3.4.1. Equipment cost

Equation (8)–(11) can be used to estimate the bare module costs, C_{BM} for each equipment or unit operation. Specifically, Equation (8) is used for compressors, Equation (9) for distillation trays, and Equation (10) for flash drums, the distillation column, pumps, and heat exchangers. The calculation of C_{BM} involves various factors and coefficients, including the purchase cost, C_P, according to Equation (11), the material factor, F_{BM}, as listed in Table (A.2), the tray factor, F_q, is the pressure factor, F_P,

Table 1
Summarised specification of unit operations.

Unit operations	Specifications
Compressors	A centrifugal compressor with an isentropic efficiency of 85%, and a maximum allowable discharge temperature of 750 °C.
Pumps	A centrifugal pump with a mechanical efficiency of 90%
Reactor	A tubular fixed bed reactor with a residence time of 30 s (Stoica et al., 2015; Klier, 1982). The reactor is packed with Raschig rings, which results in a bed porosity of about 0.72 (Jurtz, 2014). The $Cu/ZnO/Al_2O_3$ catalyst has a space–time yield of 0.721 kg methanol.h^{-1} per kg catalyst (Saito et al., 1995; Bukhtiyarova et al., 2017), and a density of 1300 kg.m^{-3}. It is also assumed that the catalyst has a lifespan of 4 years (Pérez-Fortes et al., 2016; Nieminen et al., 2019) and cost 60 USD.kg^{-1}.
Distillation column	A sieve tray-type distillation column.
Flash drum	A vertical geometry flash drum
Heat exchanger	A counter-current U-tube heat exchanger

and the bare module cost coefficients, B_1 and B_2, which can be found in Table (A.3). Additionally, the purchase cost coefficients, k_1 and k_2, are specified in Table (A.4). Finally, the sizing unit of the specific unit operation is denoted by A, which can represent power, watts (for compressor, pump, and heater/cooler), area, m^2 (for heat exchangers, and trays), or volume, m^3 (for the reactor, flash drum, distillation column, reboiler, and condenser).

$$C_{BM} = C_P F_{BM} \tag{8}$$

$$C_{BM} = C_P N_t F_{BM} F_q \tag{9}$$

$$C_{BM} = C_P(B_1 + B_2 F_{BM} F_P) \tag{10}$$

$$\log_{10} C_P = k_1 + k_2 \log_{10} A + k_3 (\log_{10} A)^2 \tag{11}$$

Equation (12)–(13) estimates the pressure factor, F_P. The former is used for heat exchangers and pumps, while the latter is applied to pressure vessels such as flash drums and distillation columns for which the thickness, θ, is greater than 0.0063 m. If $F_P < 1$, then $F_P \cong 1$ applies, meaning$\theta < 0.0063$ m. Where P_{Bg} is barg pressure in the vessel (i.e., pressure in the vessel minus 1 bar pressure), D is the diameter of the vessel, and C_1, C_2 as well as C_3 are pressure factor coefficients, which are given in Table (A.5).

$$\log_{10} F_P = C_1 + C_2 \log_{10} P_{Bg} + C_3 (\log_{10} P_{Bg})^2 \tag{12}$$

$$F_P = 158.73016 \left[\frac{D(P_{Bg} + 1)}{2[850 - 0.6(P_{Bg} + 1)]} + 0.00315 \right] \tag{13}$$

Equation (14) estimates the tray factor, F_P, which is applicable for tray numbers, $N_t < 20$, otherwise, $F_q = 1$ for $N_t \geq 20$.

$$\log_{10} F_q = 0.4771 + 0.08516 \log_{10} N_t - 0.3473 \log_{10} N_t{}^2 \tag{14}$$

To compute the bare module costs, C_{BM}, using the purchase cost, C_P, Equation (8)–(11), it is necessary to ensure that the sizing unit, A, falls within the limits specified for each unit operation (i.e., $A_{min} \leq A \leq A_{max}$). If $A < A_{min}$, then $A \cong A_{min}$ is used to estimate C_P or C_{BM} using Equation (8)–(11). On the other hand, if $A > A_{max}$, then A_{max} is used to compute C_P or C_{BM} using Equation (8)–(11) and for the given A, C_P or C_{BM} must be calculated using the cost-to-size model, Equation (15). Where $\prime\prime$ is the exponential value unique to the unit operation, Table (A.6) (Remer and Chai, 1993), where subscripts 1 and 2 indicate conditions of the two different sizes.

$$(Cost_2/Cost_1) = (Size_2/Size_1)^{\prime\prime} \tag{15}$$

It should be noted that the bare module costs, C_{BM}, which are determined using Equation (8)–(11), were originally estimated for the year 2001 (Richard et al., 2018). These costs are adjusted to account for inflation up to 2022 using the Chemical Engineering Plant Cost Index (CEPCI) for 2001 (394.3) and January 2022 (797.6), as specified in Equation (16)(Maxwell, 2022; Updating, 2002; Mignard, 2014). Here, subscripts 1 and 2 represent the values for the years 2001 and 2022, respectively.

$$Cost_2/Cost_1 = CEPCI_2/CEPCI_1 \tag{16}$$

The bare material factor, F_{BM}, is dependent on the design material. Generally, unit operations are less expensive to construct using carbon steel, but in situations where corrosion is a concern stainless steel or steel cladding may be utilised. Table (A.2) provides the bare material factors for both operating, F_{BM} and base, F^o_{BM} conditions.

In addition to considering the bare cost of unit operations, the grassroots costs of wastewater treatment (in this case, river water filtration) is also taken into account through Equation (17) considered. Equation (17), which applies for water flowrate limit, $0.01 < q_w(m^3.s^{-1}) < 10$. Where $V_{AW}(m^3)$ is the annual water usage; $C_{fuel}(USD.GJ^{-1})$ is the fuel cost, which depends on the fuel source powering the process. While **Ulrich & Vasudevan** (Ulrich and Vasudevan, 2006) provide an energy data report that can be used to estimate, C_{fuel}, however for simplicity, it is assumed $C_{fuel} \cong 3.31836\ USD.GJ^{-1}$.

$$C_{BM,WT} = \left[\left(0.00005 + \frac{2.0 \times 10^{-7}}{q_w} \right) CEPCI_2 + 0.002 C_{fuel} \right] V_{AW} \tag{17}$$

3.4.2. Operating cost

3.4.2.1. Processing cost. The utility cost, $C_{UT} = C_E Q_{AE}$, is taken to be the electricity cost, and the process cost for wastewater treatment, C_{WT}, is estimated using Equation (18) (Ulrich and Vasudevan, 2006). Where Q_{AE} (KWh) is the electricity usage for pumping and compression, while $C_E(USD.KWh^{-1})$ is the electricity unit cost for manufacturing companies, which is taken as $C_E = 0.119\ USD.KWh^{-1}$ for Finland (Finland Statistics, 2021). The raw material cost, C_{RM}, which represents the cost of carbon dioxide and hydrogen gas required for the process, can also be estimated using a similar procedure as the electricity cost. Specifically, the cost of each raw material component is the product of its unit cost and the amount needed. The unit cost of carbon dioxide and hydrogen gas is taken as $0.0583\ USD.kg^{-1}$ and $3\ USD.kg^{-1}$, respectively.

$$C_{WT} = \left[\left(0.0001 + \frac{2.0 \times 10^{-7}}{q_w} \right) CEPCI_2 + 0.002 C_{fuel} \right] V_{AW} \tag{18}$$

3.4.2.2. Operating labour cost. The operating labour cost, C_{OL}, Equation (19), is estimated based on the number of operators needed per shift, N_{OL}, Equation (20), and annual labour wage, C_{WG}. Where N_{PS}, is the number of particulate solids processing steps, N_{SD} is the number of shifts per day and $N_{np} = \Sigma_{i=1}^{n} \text{Unit operations}$ is the sum of nonparticulate processing steps such as compression, heat transfer processes, mixing, and reaction. In this work, N_{np} constitute compressors, towers, reactors, exchangers, and wastewater treatment units.

$$C_{OL} = C_{WG} N_{OL} N_{SD} \tag{19}$$

$$N_{OL} = \left(6.29 + 31.7 N_{PS}^2 + 0.23 N_{np} \right)^{0.5} \tag{20}$$

4. Methodologies

4.1. Design of experiment

A preliminary investigation of the values of process variables, as reported in literature, is performed to implement the Design of Experiment (DOE) for a given plant size of the designed plant model, Fig. 2. Therefore, to avoid hydrothermal sintering and deactivation of catalyst due to liquid formation (Peng et al., 1997), variation of pressure (35–148 atm), and temperature (200–300 °C) was simulated for a two-phase RGibbs reactor with the assumption of an entirely gaseous output. The result shown in Fig. 3 indicate the formation of liquid from 99 atm, thus the DOE was developed for plant size of 40–1500 $kt.yr^{-1}$ pressure (35–98 atm), and temperature (200–300 °C).

A three-variable-five-level (i.e., $\mathscr{K} = 3$) Central Composite Design (CCD) of nine (9) centre points (i.e., $n_c = 9$) was adopted, resulting in twenty-four (24) simulation runs (N) for each response or objective considered, as given by Equation (21). The design analyses the contribution of the three variables in terms of linear, quadratic, and interaction effects on responses through the generalised second-order polynomial regression model using coded values (x), as given by Equation (23). Equation (22) and Table 2 shows the relationship between x and actual values (ξ) of the specified variables for the DOE (Rakić et al., 2014). Where $\bar{\xi} = 0.5\ (\xi_{min} + \xi_{max})$; ξ_{min} and ξ_{max} are the mean, minimum, and maximum actual values of variables. The 'star points' that allow for evaluation of curvature for inscribed CCD are given by $\alpha = \pm(2^k)^{-0.25}$. The resulting process variables in the CCD are distributed over the limits illustrated in Table 2, and these limits are the upper limit,

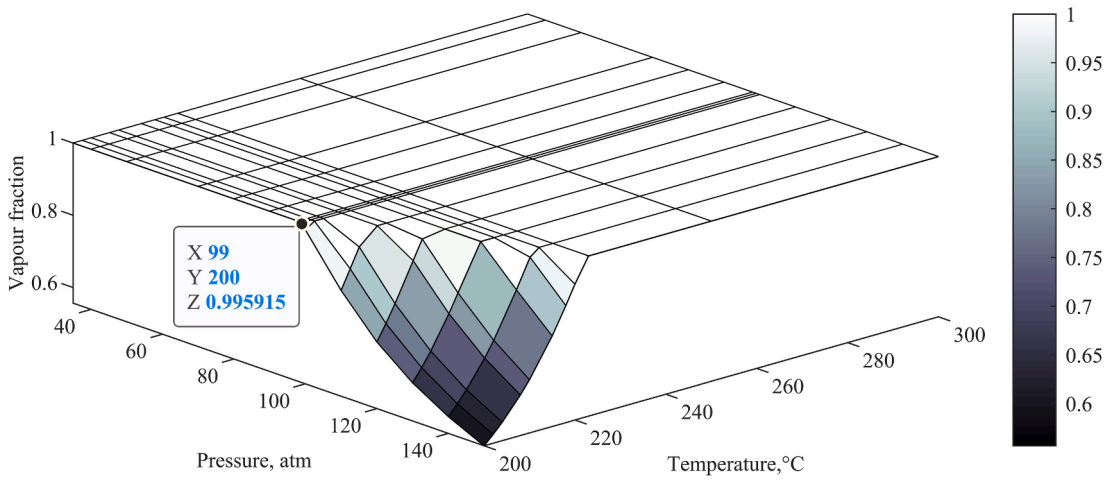

Fig. 3. Vapour fraction of reactor content at different pressure and temperature for plant model.

Table 2
Coded and actual levels of the process variables for inscribed central composite design.

Variable, unit	symbols	Coded and actual value $x_i(-1)$, lower limits	$x_i(-\alpha)$, Lower midpoints	$x_i(0)$, midpoints	$x_i(+\alpha)$, Upper midpoints	$x_i(1)$, upper limits
Plant size, kt.yr^{-1}	ξ_1	40.0000	335.9394	770.0	1204.0606	1500.0
Pressure, atm	ξ_2	35.0000	47.78000	66.50	85.230000	98.000
Temperature, °C	ξ_3	200.000	220.2698	250.0	279.73020	300.00

$+1$; upper mid-point, $+\alpha$; mid-point, 0; lower mid-point, $-\alpha$; lower limit, -1.

$$N = \mathscr{K}^2 + 2\mathscr{K} + n_c \tag{21}$$

$$x = (\xi - \bar{\xi})/\beta(\xi_{max} - \xi_{min}) \tag{22}$$

$$f(x) = \beta_0 + \Sigma_{i=1}^{n}\beta_i x_i + \Sigma_{i=1}^{n}\beta_{ii}x_i^2 + \Sigma_{i=1}^{n}\Sigma_{j=1}^{n}\beta_{ij}x_i x_j \tag{23}$$

Equation (23) models the response $f(x)$, which represents manufacturing cost, and conversion of carbon dioxide; with x_i and x_j representing the specified variables of consideration; β_0 is the model's constant; β_i is the linear term coefficient; β_{ii} is the quadratic term coefficient; β_{ij} is the interaction coefficient and n is the number of variables considered. Additionally, this equation can model the amount of carbon dioxides, carbon monoxide, methanol, water, and hydrogen gas from the reactor at different temperatures and pressures. The models are developed based on a statistical significance test of p-value < 0.05 validation hypothesis for the entire equation $f(x)$ and each variable, x.

MATLAB was used to generate the inscribed CCD design via the Central Composite Design (ccdesign) function, and Equation (23) was developed, as well as evaluated with the Fit Linear Regression Model (fitlm) function.

4.2. Optimisation of plant model

Fig. 2 depicts the designed methanol plant model, which will be optimised to determine the optimal process variables (plant size, temperature, and pressure). In this study, it is proposed that an effective optimisation approach involves simultaneously minimising manufacturing unit cost, $f(x)_1$ (USD.tonne^{-1}) and maximising the conversion of carbon dioxide, $f(x)_2$(%), as described by the multi-objective optimisation procedure, Equation (24). These two responses are statistical models developed in terms of highlighted process variables in Table 2 and as described by Equation (23) (Khor et al., 2019; Tao et al., 2019; Cheng, 1999; Abu-Reesh, 2020). In Equation (24); $G(x)$ and $H(x)$ respectively represent the vectors of nonlinear inequality and equality constraints; g and s denote constants in the linear inequality constraint; h and m are the linear equality constants, which are developed from the variables (x) lower, l and upper, u limits.

Objective

$$\text{minimise}\{f(x)_1, -f(x)_2\}$$

Subject to

$$\text{Inequality constraint} \begin{cases} G(x) \le 0 \\ gx \le s \end{cases} \tag{24}$$

$$\text{Equality constraint} \begin{cases} H(x) = 0 \\ hx = m \end{cases}$$

$$\text{Allowable limits} \quad l \le x \le u$$

Furthermore, if it is necessary to optimise these responses individually, a single objective optimisation approach can be applied using Equation (24) by remodelling it as $\text{minimise}\{\pm f(x)\}$. Equation (24) is solved using MATLAB's Solve Minimax Constraint Problem (fminimax) and Find Minimum of Constrained Nonlinear Multivariable (fmincon) optimisation toolboxes. The optimisation steps and pseudocode are highlighted in Figure (A.1) and Algorithm (1) of the appendix.

5. Results and discussion

5.1. Development of multivariable regression model

The generated inscribed CCD for the plant model is given in Table (A.19) in the appendix. Therefore, using results from the Aspen Plus simulation, the responses required for the development of Equation (23) were deduced: manufacturing unit cost, i.e., the result of Equation (7) divided by tonnes of methanol produced; and conversion of carbon dioxide, i.e., carbon dioxide reacted divided by carbon dioxide fed into the reactor. In addition to these responses, resulting carbon dioxides, carbon monoxide, methanol, water, and hydrogen gas/vapour from the reactor are also considered.

The resulting statistical models for manufacturing unit cost (USD.

Table 3
Statistical evaluation parameters for the manufacturing cost.

Process variable (coded)		Standard Error	t-statistic	Probability-value, P-value
Linear effect	Intercept,β_0	11.9377	75.7795	1.0553E-19
	Production rate,x_1	17.1899	−3.5329	0.0033
	Pressure,x_2	17.1899	−1.8180	0.0905
	Temperature,x_3	17.1899	2.0551	0.0590
Interactive effect	x_1x_2	37.7725	−0.0558	0.9563
	x_1x_3	37.7725	0.0730	0.9428
	x_2x_3	37.7725	−0.6900	0.5015
Quadratic effect	x_1^2	26.5254	3.3897	0.0044
	x_2^2	26.5254	0.6361	0.5350
	x_3^2	26.5254	−0.3804	0.7093
Model		–	–	0.0156

Table 4
Statistical evaluation parameters for the Conversion of carbon dioxide.

Process variable (coded)		Standard Error	t-statistic	Probability-value, P-value
Linear effect	Intercept,β_0	1.5198E-04	1.0898E + 03	6.6271E-36
	Production rate,x_1	2.1884E-04	−0.0023	0.9982
	Pressure,x_2	2.1884E-04	276.4593	1.4477E-27
	Temperature,x_3	2.1884E-04	−324.8259	1.5154E-28
Interactive effect	x_1x_2	4.8088E-04	−0.0027	0.9979
	x_1x_3	4.8088E-04	0.0060	0.9953
	x_2x_3	4.8088E-04	−37.0865	2.2189E-15
Quadratic effect	x_1^2	3.3769E-04	0.1966	0.8469
	x_2^2	3.3769E-04	−18.7169	2.6366E-11
	x_3^2	3.3769E-04	47.4991	7.1253E-17
Model		–	–	2.7900E-27

Table 5
Statistical evaluation parameters for the manufacturing cost (2).

Process variable (coded)		Standard Error	t-statistic	Probability-value, P-value
Linear effect	Intercept,β_0	8.3386	108.6479	5.1794E-28
	Production rate,x_1	15.2875	−3.9726	0.0008
	Pressure,x_2	15.2875	−2.0442	0.0550
	Temperature,x_3	15.2875	2.3109	0.0322
Quadratic effect	x_1^2	23.5852	3.8163	0.0012
Model		–	–	0.0002

Table 6
Statistical evaluation parameters for the Conversion of carbon dioxide (2).

Process variable (coded)		Standard Error	t-statistic	Probability-value, P-value
Linear effect	Intercept,β_0	0.0001	1370.2422	1.2686E-46
	Pressure,x_2	0.0002	313.0429	4.4073E-35
	Temperature,x_3	0.0002	−367.8099	2.4211E-36
Interactive effect	x_2x_3	0.0004	−41.9942	2.0446E-19
Quadratic effect	x_2^2	0.0003	−21.1927	3.5355E-14
	x_3^2	0.0003	53.7929	2.4528E-21
Model		–	–	1.9700E-36

tonne^{-1}) and conversion of carbon dioxide are given by Equations (25) and (26) respectively. Following the validation hypothesis of p-value $<$ 0.05, both Equation (25) (p-value = 0.0156) and Equation (26) (p-value = 2.79E-27) were found to be significant, as given in Tables 3 and 4. Considering the details of Equation (25) from Table 3, its intercept, β_0, linear, x_1 and quadratic x_1^2 effects of plant size are the significant variables observed. This implies the manufacturing cost of the methanol plant model, Fig. 2, is mainly affected by the plant size. Therefore, Equation (25) can be redeveloped in terms of the reported significant variable, x_1 as given by Equation (27). However, since all linear effects (especially temperature) are not far off from p-value $<$ 0.05, they can be also considered. The resulting new model has a better fit than the previous model, i.e., p-value (0.0002) $<$ p-value (0.0156) of Table 5 and 3, respectively. Furthermore, temperature, x_2 was found to be significant, Table 5. The significant effect of plant size on manufacturing cost is expected because, as reported in literature, manufacturing cost reduces with plant size (Nguyen and Prince, 1996; Haldi and Whitcomb, 1967). This fact is indicative of the negative coefficient of the significant linear effect on production rate, x_1, in Equations (25) and (27). However, this effect is not entirely linear, as manufacturing cost also increases significantly with the quadratic effect for plant size, x_1^2. The respective negative and positive coefficients of x_1 and x_1^2 may imply that although manufacturing cost decrease with increased plant size, beyond a certain limit, larger plant sizes can result in higher manufacturing costs.

Furthermore, based on the respective negative and positive coefficients of pressure and temperature in Equation (27), as well as observation of Table 5, the manufacturing cost will reduce slightly with increased pressure (due to its insignificance in the model), and increase significantly with increased temperature.

$$f(x)_1 = 904.6312 - 60.7309x_1 - 31.2505x_2 + 35.3275x_3 - 2.1086x_1x_2 + 2.7578x_1x_3 - 26.0621x_2x_3 + 89.9135x_1^2 + 16.8723x_2^2 - 10.0914x_3^2 \quad (25)$$

$$f(x)_2 = 0.1656 - 5.0185 \times 10^{-7}x_1 + 0.0605x_2 - 0.0711x_3 - 1.3169 \times 10^{-6}x_1x_2 + 2.8962 \times 10^{-6}x_1x_3 - 0.0178x_2x_3 + 6.6399 \times 10^{-5}x_1^2 - 0.0063x_2^2 + 0.0160x_3^2 \quad (26)$$

Equation (26) and Table 4 shows that temperature and pressure have the expected influence on conversion of carbon dioxide. Specifically, the linear effect of pressure, x_2 and temperature, x_3, as well as their interaction, x_2x_3 together with their quadratic effect, x_2^2 and x_3^2, significantly influence conversion of carbon dioxide. Therefore, redeveloping Equation (26) in terms of these significant variables resulted in a better model, Equation (28) i.e., p-value (1.97E-36) < p-value (2.79E-27) as given in Table 6. Furthermore, the positive and negative linear coefficients of pressure and temperature in Equations (26) and (28) may imply that an increase in pressure linearly increases the conversion of carbon dioxide, although this increase is limited by the negative interaction effect of pressure and temperature, x_2x_3, and the negative quadratic effect of pressure, x_2^2. On the other hand, increasing temperature linearly decreases conversion of carbon dioxide, which is further enhanced by the negative interaction effect of pressure and temperature, x_2x_3, but limited by the positive quadratic effect of pressure, x_2^2.

$$f(x)_1 = 905.976 - 60.7309x_1 - 31.2505x_2 + 35.3275x_3 + 90.0091x_1^2 \quad (27)$$

$$f(x)_2 = 0.1656 + 0.0605x_2 - 0.0711x_3 - 0.0178x_2x_3 - 0.0063x_2^2 + 0.0160x_3^2 \quad (28)$$

In addition to Equation (27)–(28), significant statistical models (with a p-value < 0.05) that predict methanol formation rate, R_{CH_3OH}(kmole.kgcat^{-1}hr^{-1}), carbon monoxide formation rate, R_{CO}(kmole.kgcat^{-1}hr^{-1}), methanol, n_{MEOH}, carbon dioxide, n_{CO2}, carbon monoxide, n_{CO}, water, n_{H2O}, and hydrogen gas, n_{H2} mole fraction from the Gibbs reactor are respectively given by Equation (29)–(35). These models are all significantly influenced by reaction pressure and temperature, except for reaction rate models (R_{CH_3OH} and R_{CO}), where the production rate, x_1 influences the rate linearly and interactively with pressure as well as temperature. However, for mole fraction models (n_{CH_3OH}, n_{CO2}, n_{CO}, n_{H2O} and n_{H2}), the influence of production rate, x_1, is insignificant.

$$R_{CH_3OH} = 38232 + 40057x_1 - 21901x_2 + 26049x_3 - 20122x_1x_2 + 25199x_1x_3 - 15457x_2x_3 + 11167x_2^2 + 8714.8x_3^2 \quad (29)$$

$$R_{CO} = 2876.4 + 2740.8x_1 - 94.994x_2 + 79.418x_3 - 80.272x_1x_2 + 80.345x_1x_3 - 69.84x_2x_3 + 75.616x_2^2 \quad (30)$$

$$n_{CH_3OH} = 0.0751 + 0.0324x_2 - 0.0432x_3 - 0.0141x_2x_3 - 0.0010x_2^2 + 0.0098x_3^2 \quad (31)$$

$$n_{CO2} = 0.3614 + 0.0081x_2 - 0.0302x_3 + 0.0203x_2x_3 - 0.0064x_2^2 - 0.0234x_3^2 \quad (32)$$

$$n_{CO} = 0.0284 - 0.0181x_2 + 0.0486x_3 - 0.0218x_2x_3 + 0.0080x_2^2 + 0.0268x_3^2 \quad (33)$$

$$n_{H2O} = 0.0723 + 0.0326x_2 - 0.0429x_3 - 0.0138x_2x_3 - 0.0015x_2^2 + 0.0098x_3^2 \quad (34)$$

$$n_{H2} = 0.4630 - 0.0549x_2 + 0.0677x_3 + 0.0293x_2x_3 - 0.0230x_3^2 \quad (35)$$

5.2. Optimisation of designed plant model

Having developed models for manufacturing unit cost and conversion of carbon dioxide, it is assumed that adequate optimisation of the designed plant can be achieved with simultaneous optimisation of these models. This can be performed in MATLAB using, either Equations (25) and (26) or Equations (27) and (28), in collaboration with the lower, l, and upper, u limits of the coded variables, x, as given by Equation (36).

Objective

$$\text{minimise}\{f(x)_1, -f(x)_2\}$$

Subject to

$$\text{Allowable limits} \quad -1 \le x \le 1 \quad (36)$$

The resulting optimal values: process variables – plant size, x_1= 0.3351(ξ_1 = 1029.2377 kt.yr^{-1}), pressure, x_2= 0.1760(ξ_2 = 72.0429 atm), and temperature, x_3= −1.0000(ξ_3 = 200 °C); process responses – manufacturing unit cost, $f(x)_1$= 847.4814 USD.tonne^{-1}, Fig. 4a, and conversion of carbon dioxide, $f(x)_2$= 0.2663, Fig. 4b, were estimated using the fminimax toolbox. Note that while the optimal temperature may be acceptable (because temperature is statistically significant for both models), the optimal plant size and pressure may need further investigation. This inference was investigated by performing single-objective optimisation on manufacturing unit cost (i.e., minimise$\{f(x)_1\}$) and conversion of carbon dioxide (i.e., minimise$\{-f(x)_2\}$), Equation (37) using the fmincon toolbox.

Objective

$$\text{minimise}\{\pm f(x)\}$$

Subject to

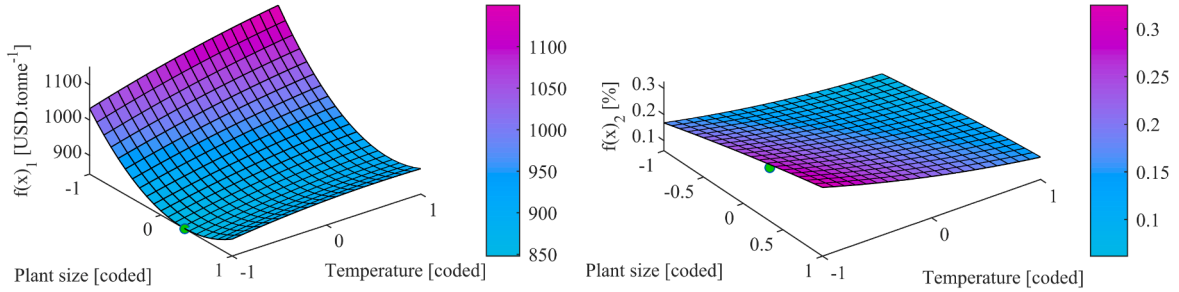

a. Manufacturing unit cost b. Conversion of carbon dioxide

Fig. 4. Changes in objectives of the plant model with plant size, pressure, and temperature.

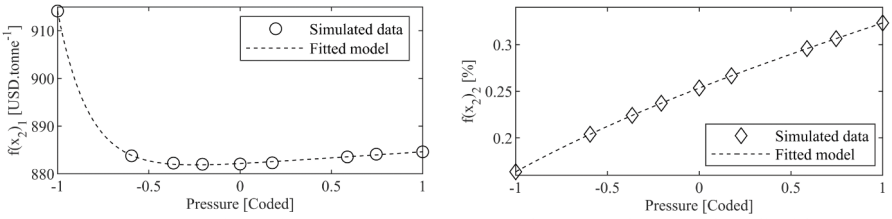

a. Manufacturing unit cost b. Conversion of carbon dioxide

Fig. 5. Changes in plant objectives with pressure at optimal plant size, and temperature.

Table 7
Final optimal values of process variables and responses.

Process variable	Optimal coded, x (Actual,ξ) value
Plant size	0.3351 (1029.2377 kt.yr^{-1})
Pressure	−0.2451 (58.7794 atm)
Temperature	−1.0000 (200 °C)
Manufacturing unit cost	881.9161 USD.tonne^{-1}
Conversion of carbon dioxide	0.2341

Table 8
Constants for LHHW kinetic model for the formation of methanol and carbon monoxides.

Pressure constants	Values
K_{CH_3OH}(bar^{-1})	$10^{3066/T-10.592}$
K_{CH_3OH}(unitless)	$10^{-2073/T-2.029}$
K_1(kmoles.kgcat^{-1}s^{-1}bar^{-2})	−0.4745
K_2(unitless)	−2.0219E-04
K_3(bar$^{-0.5}$)	10.6579
K_4(bar^{-1})	−0.0010
K_5(kmoles.kgcat^{-1}s^{-1}bar^{-1})	−7.5925E-08
RMSE	0.0012

Allowable limits $-1 \leq x \leq 1$ (37)

Results for the optimisation of manufacturing unit cost, $f(x)_1$= 847.4814 USD.tonne^{-1} showed thatx_1 = 0.3351, x_2= 0.1760, and x_3 = -1.0000. Similarly, for conversion of carbon dioxide, $f(x)_2$= 0.3248, x_1= −0.9971, x_2= 1.0000, andx_3 = -1.0000 were deduced. Notably, the estimated optimal temperature, x_3= −1.0000(ξ_3 = 200 °C) was the same for all optimisation routes, which confirms the earlier highlighted inference. This temperature value corresponds to literature reports (Rosha et al., 2021; Lo and Wu, 2019) for the Cu/ZnO/Al_2O_3 catalyst.

Furthermore, plant size, x_1 was found to be significant in the manufacturing unit cost model, $f(x)_1$ and its optimal, x_1= 0.3351 was the same for the multi-objective optimisation, Equation (36), as well as for the single-objective optimisation, Equation (37), this result is taken as the true optimal. However, pressure, x_2 was significant in the conversion of carbon dioxide model, $f(x)_2$, and its optimal was different for multi-objective optimisation, x_2= 0.1760 and single-objective optimisation, x_2= 1.0000. Thus, its optimal value is uncertain. To accurately determine the optimal pressure, new models for manufacturing unit cost, Equation (38) and conversion of carbon dioxide, Equation (39) by varying the pressure, x_2 (i.e., Fig. 5a and 5a respectively) at the true optimal plant size, x_1= 0.3351, as well as temperature, x_3= −1.0000 were developed, and optimised. The true optimal pressure, x_2= −0.2451 (ξ_2 = 58.7794 atm) was then determined by applying Equation (37) with Equation (38) or alternative by applying Equation (36) with Equation (38) and (39).

$$f(x_2)_1 = 0.4630e^{-5.7790x_2} + 882.1e^{0.0029x_2} \quad (38)$$

$$f(x_2)_2 = 0.2989e^{0.1432x_2} - 0.0455e^{-0.7403x_2} \quad (39)$$

The optimal pressure that was deduced is within the value range reported in literature (Borisut and Nuchitprasittichai, 2019). Finally, Table 7 summarises the true optimal values for the methanol plant model.

The accuracy of the optimisation procedure was validated by simulating the plant model at the deduced optimal conditions given in Table 7 and comparing its response with results of the manually calculated responses – $f(x)_1$= 882.0508 USD.tonne^{-1} and $f(x)_2$ = 0.2341. The negligible difference between the results of responses shows the optimisation procedure is adequate.

5.3. LHHW kinetic for designed plant model

Considering simulations were performed at various pressures for the optimal plant size and temperature, the resulting data can be used to investigate, as well as develop the Langmuir-Hinshelwood-Hougen-Watson (LHHW) reaction kinetics equivalent to the Gibbs model employed in this study. Equations (40) and (41), are frequently used to describe the LHHW kinetics (Ghosh et al., 2021; Portha et al., 2017). Note that the kinetics for carbon dioxide has been neglected, since

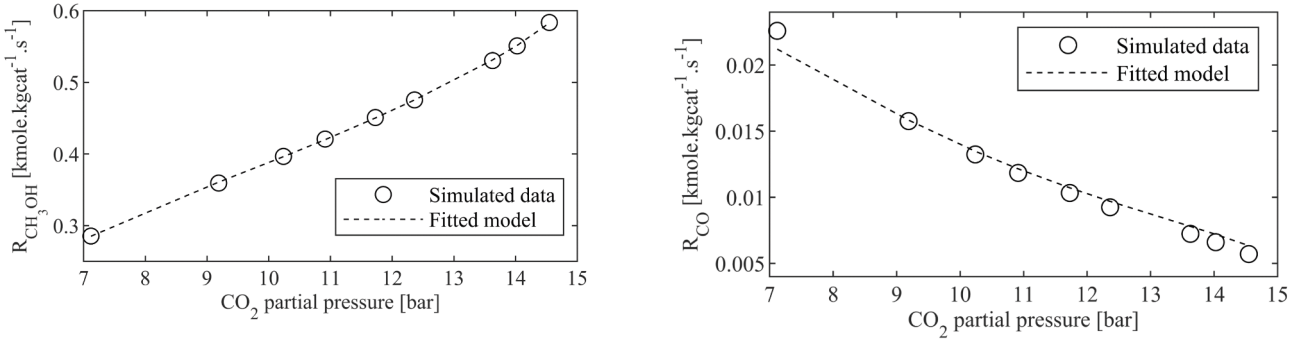

a. Methanol formation rate b. Carbon monoxide formation rate

Fig. 6. LHHW kinetic for methanol and carbon monoxide formation rate.

Table 9
Summarised cost composition for designed plant model at optimal condition.

Compositional units	Cost (USD)	Percentage (%)
Bare module cost (CBM)	**121026768.7**	**100**
Compression unit	16927912.45	13.9869
Pumping unit	550470.8722	0.45483
Heat exchanger unit	29901498.45	24.7065
Heater unit	–	0.0000
Reaction unit	50705729.71	41.8963
Phase separation unit	4330622.521	3.5782
Distillation unit	17643334.16	14.578
Wastewater treatment unit	967200.485	0.7992
Operating cost	**674257111.8**	**100**
Raw material	608079440.4	90.2000 (100*)
Carbon dioxide	75482849.69	12.4000*
Hydrogen gas	532596590.7	87.6000*
Electricity	62395123.42	9.2500 (100*)
Compression	61209527.9	98*
Pumping	1185595.51	1.9000*
Heater	–	–
Wastewater treatment	1792468.036	0.2700
Labour	1,990,080	0.3000
Grassroots cost	174249884.7	–
Manufacturing cost	828,510,959	–
Manufacturing unit cost	882.0508	–
District heating saving	35175387.74	–

Table 10
Summarised design details on the reactor, flash drums, and distillation column.

Parameters (unit)	Values
Reactor	
Fed reactant volume, V_{fr} (m^3)	172.93726
Catalyst volume, V_{cat} (m^3)	174.2180409
Total volume, V_{rxn} (m^3)	346.6121
Diameter, D_r (m)	4.7956
Conversion of carbon dioxide	0.2341
Flash drum (FD-1)	
Residence time, t_{fd}(hr)	10.662/60
Volume, V_{fd} (m^3)	51.3862
Diameter, D_{fd}(m)	2.7935
Flash drum (FD-2)	
Residence time, t_{fd}(hr)	3.612/60
Volume, V_{fd} (m^3)	18.8691
Diameter, D_{fd}(m)	2.0003
Distillation column	
Numbers of trays	11
Residence time, t_{dc}(hr)	10.7558
Volume, V_{dc} (m^3)	214.2978
Diameter, D_{dc}(m)	6.4284
Reflux ratio,R_D	0.6002
Volume of condenser (m^3)	296.0250
Volume of reboiler (m^3)	210.5804

carbon monoxide is absent in the feedstock, as such no formation of carbon dioxide from it. Where K_{CH_3OH}, and K_{CH_3OH} are temperature (T, Kelvins) dependent constants. While K_1, K_2, K_3, K_4 and K_5 are curve-fitted pressure constants deduced from the simulation data, as given in Table 8. These constants were deduced using the lsqcurvefit toolbox in MATLAB through the minimisation of the Root Mean Squared Error (RMSE), Equation (42) between the simulated (y) and curve-fitted ($\hat{y}$) product formation rate (R_{CH_3OH} and R_{CO}). Where $\mathscr{N} = 9$ is the number of varied pressure simulation runs, and $\mathscr{P} = 2$ is the number of dependent variables in the models. Fig. 6 illustrates the formation rate of methanol, Fig. 6a, and carbon monoxide, Fig. 6b as a function of the partial pressure of carbon dioxide in the reactor.

$$R_{CH_3OH} = K_1 P_{CO_2} P_{H_2} \left(1 - \frac{P_{H_2O} P_{CH_3OH}}{K_{CH_3OH} P_{H_2}^2 P_{CO_2}}\right) \left(1 + K_2 \frac{P_{H_2O}}{P_{H_2}} + K_3 P_{H_2}^{0.5} + K_4 P_{H_2O}\right)^{-3} \tag{40}$$

$$R_{CO} = K_5 P_{CO_2} \left(1 - \frac{K_{CO} P_{H_2O} P_{CO}}{P_{H_2} P_{CO_2}}\right) \left(1 + K_2 \frac{P_{H_2O}}{P_{H_2}} + K_3 P_{H_2}^{0.5} + K_4 P_{H_2O}\right)^{-1} \tag{41}$$

$$RMSE = \sqrt{\frac{\Sigma (y - \hat{y})^2}{\mathscr{N} - \mathscr{P} - 1}} \tag{42}$$

The adequacy of this result suggests that the LHHW kinetic reactor, as described in literature (Van-Dal and Bouallou, 2013; Luyben, 2010; Samiee and GhasemiKafrudi, 2045); can serve as an alternative to the Gibbs reactor. As expected, increasing the partial pressure of carbon dioxide, as shown in Equations (40) and (41) and illustrated in Fig. 6, favours methanol formation rate, R_{CH_3OH}, Fig. 6a, but negates the water–gas-shift reaction, i.e., the carbon monoxide formation rate, R_{CO}, Fig. 6b.

5.4. Evaluation of plant model at optimal conditions

Having calculated the designed plant optimal as shown in Table 7, simulations were carried out at these conditions to compare the resulting manufacturing unit cost, Table 9 as well as the conversion of carbon dioxide, Table 10. The simulation results validate the accuracy of the calculated optimal conditions. In addition, the cost compositions at optimal conditions were evaluated. While the methanol manufacturing

Table 11
Evaluated exponential value and goodness of fit for important plant costs.

Parameters (USD)	Exponential value,$\mathscr{n}$	R^2-Value
Bare module cost	0.7630	0.9989
Grassroots cost	0.7398	0.9993
Manufacturing cost	0.9378	0.9994

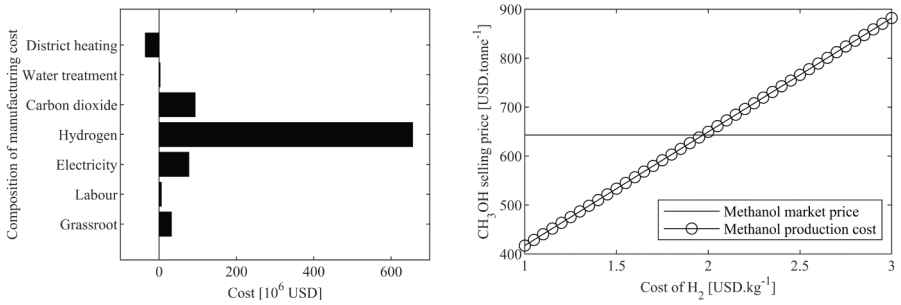

a. Composition of manufacturing cost

b. Profitability evaluation from manufacturing cost

Fig. 7. Evaluation of manufacturing cost for designed plant model.

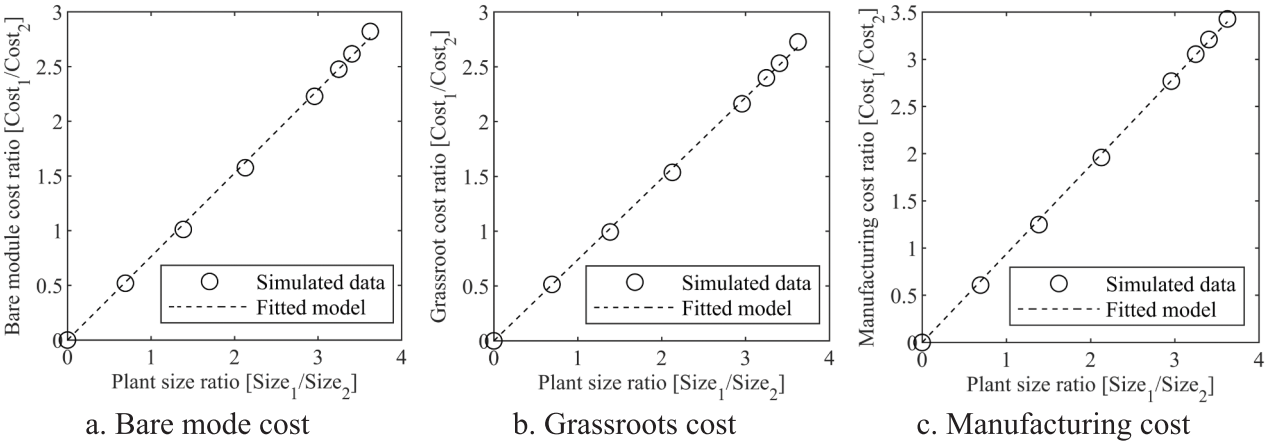

Fig. 8. Illustration of evaluated exponential value for important plant costs.

cost can be described by Equation (7), details on other cost compositions such as bare module and operating costs are given in Table 9. Furthermore, design details on the reactor, flash drum, and distillation column highlighted in Section (1.1) of the appendix are summarised in Table 10.

The result in Table 9 indicates that the reaction unit constitutes the highest cost (41.8963%) incurred in setting up the plant. This is followed by the heat exchanger (24.7065%), distillation (14.578%), and compression (13.9869%) units. The high cost of reactor and heat exchanger units is due to the large volume of gaseous feed stream caused by high temperature and the cost of vessel construction due to the high pressure requirement. The cost implication of a high-pressure vessel is accounted for by the pressure factors, Equation (12) and (13). While the cost of the distillation unit is mainly due to the large volume of its feed stream caused by high temperature and low pressure.

Furthermore, considering the operating cost, the raw materials as expected constitute the highest cost (90.2%) for which the cost of hydrogen is highest (87.6%). Therefore, the cost of hydrogen constitutes the bulk of the manufacturing cost, Fig. 7a.

$$C_{OM} = 218364602.2C_{H_2} + 173417152.5 \quad (43)$$

It implies the cost of hydrogen is the primary cost-determining factor in methanol production, as such its profitability, as reported in literature (Atsonios et al., 2016; Leonzio, 2018; Abbas et al., 2022). Therefore Equation (7) can be disintegrated to relate the unit cost of hydrogen gas, C_{H_2} to the deduced optimal conditions, as given by Equation (43) for a CECPI value of January 2022. Considering the unit cost of hydrogen gas used in this simulation is $C_{H_2} = 3$ USD. Kg^{-1} and the current market price of methanol is 643 USD. $tonne^{-1}$. Therefore, as illustrated in Fig. 7b in collaboration with Equation (43), the designed plant model will be profitable for hydrogen unit cost of < 2 USD. Kg^{-1}. The reduction of hydrogen unit cost can be actualised by future innovation and improvement of the efficiency of electrolyser used in electrolysis of water (Song et al., 2022; Idriss, 2020) or alternative splitting of water to release hydrogen gas without electricity or heat (Erogbogbo et al., 2013).

5.5. Estimation of the exponential value of the cost-to-size model

In certain situations, it might be necessary to quickly estimate important costs for methanol production plants such as bare module, grassroots, and manufacturing costs for various plant sizes when comprehensively calculated cost value of one plant size is known. Equation (15) can be applied to unit operations for this purpose, but the unique exponential value, n, must be determined.

$$\log(Cost_2/Cost_1) = n\log(Size_2/Size_1) \quad (44)$$

To do this, the fitlm function in MATLAB is used in conjunction with the linearised form of Equation (15), which is given by Equation (44). The unique exponential values, n, for the bare module, grassroots, and manufacturing costs for the designed plant model at optimal conditions are determined and presented in Table 11 and illustrated by Fig. 8.

6. Conclusion

In conclusion, a methanol plant model was proposed and designed using condtions for Finland as a case study, and simulated in Aspen Plus software using appropriate fluid packages, specifically the PENG-ROB, Steam-TA, and NRTL property packages. To optimise the plant model, an inscribed Central Composite Design (CCD) type of Design of Experiment (DOE) was developed for three process variables namely plant size, process pressure, and temperature, and two process responses, manufacturing unit cost and conversion of carbon dioxide. The CCD was developed based on a preliminary simulation, and the following data range for process variables were utilised: 40–1500 $kt.yr^{-1}$ plant, 35–98 atm pressure and 200–300 °C temperature. Statistical models were developed from the CCD and validated based on the p-value < 0.05 significance test. These statistical models were then used for the optimisation of the plant model, through the combination of single-objective and multi-objective optimisation procedures. The resulting optimal values for process variables (plant size of 1029.2377 kt.yr-1, pressure of 58.7794 atm, and temperature of 200 °C) and process responses (manufacturing unit cost, $f(x)_1 = 881.9161$ USD.$tonne^{-1}$ and conversion of carbon dioxide, $f(x)_2 = 0.2341$) were deduced.

The Langmuir-Hinshelwood-Hougen-Watson (LHHW) kinetic model equivalent to the Gibbs model used in the simulation was developed using data from simulations performed at different pressures for optimal plant size and temperature. The developed LHHW kinetic model showed an excellent fit, with a Root Mean Squared Error (RMSE) of 0.0012. Additionally, the cost compositions at optimal conditions were evaluated, revealing that the reaction unit accounted for the bulk (41.8963%) of the bare module cost, and the cost of hydrogen gas was the highest operating and manufacturing cost, thus constituted the main cost-determining factor of the methanol plant. Therefore, the manufacturing cost was remodelled to relate the unit cost of hydrogen gas, C_{H_2}, for the deduced optimal conditions. This model was used to assess the profitability of the plant in comparison with the current market price of methanol (643 USD. $tonne^{-1}$), indicating that the plant would be profitable at a hydrogen cost of < 2 USD. Kg^{-1}.

Finally, the unique exponential values of the cost-to-size model for the bare module ($n = 0.7630$), grassroots ($n = 0.7398$), and manufacturing costs ($n = 0.9378$) were deduced for the designed plant model at the optimal conditions with an excellent R^2-value of 0.9989,

0.9993 and 0.9994, respectively.

Declaration of Competing Interest

The authors declare that they have no known competing financial interests or personal relationships that could have appeared to influence the work reported in this paper.

Data availability

Data will be made available on request.

Acknowledgment

This work was supported by the Department of Energy, Lappeenranta-Lahti University of Technology, and the Internal Grant Agency (IGA/CebiaTech/2023/004) of Tomas Bata University.

Extra information

Note that sample results and calculation steps for a given simulation scenario are found in the supplementary data files.

Appendix A. Supplementary data

Supplementary data to this article can be found online at https://doi.org/10.1016/j.ces.2023.118888.

References

Abbas, A., Qadeer, K., Al-Hinai, A., Tarar, M.H., Qyyum, M.A., Al-Muhtaseb, A.H., Abri, R.A., Lee, M., Dickson, R., 2022. Process development and policy implications for large scale deployment of solar-driven electrolysis-based renewable methanol production. Green Chemistry 24 (19), 7630–7643.

Abu-Reesh, I.M., 2020. Single-and multi-objective optimization of a dual-chamber microbial fuel cell operating in continuous-flow mode at steady state. Processes 8 (7), 839.

Aimiuwu, G., Osagie, E., Omoregbe, O., 2022. Process simulation for the production of methanol via CO2 reforming of methane route. Chemical Product and Process Modeling 17, 69–79. https://doi.org/10.1515/CPPM-2020-0049/MACHINEREADABLECITATION/RIS.

Albuquerque, F.D.B., Maraqa, M.A., Chowdhury, R., Mauga, T., Alzard, M., 2020. Greenhouse gas emissions associated with road transport projects: current status, benchmarking, and assessment tools. Transportation Research Procedia 48, 2018–2030. https://doi.org/10.1016/J.TRPRO.2020.08.261.

Andersson, J., Grönkvist, S., 2019. Large-scale storage of hydrogen. Int J Hydrogen Energy 44, 11901–11919. https://doi.org/10.1016/J.IJHYDENE.2019.03.063.

Atsonios, K., Panopoulos, K.D., Kakaras, E., 2016. Investigation of technical and economic aspects for methanol production through CO2 hydrogenation. Int J Hydrogen Energy 41, 2202–2214. https://doi.org/10.1016/J.IJHYDENE.2015.12.074.

Bakar, S.H.A., Hamid, M.K.A., Alwi, S.R.W., Manan, Z.A., 2015. Effect of Delta Temperature Minimum Contribution in Obtaining an Operable and Flexible Heat Exchanger Network. Energy Procedia 75, 3142–3147. https://doi.org/10.1016/J.EGYPRO.2015.07.648.

Ball, M., Weeda, M., 2016. The hydrogen economy—Vision or reality? Compendium of Hydrogen Energy 237–266. https://doi.org/10.1016/B978-1-78242-364-5.00011-7.

Behrens, M., 2016. Promoting the Synthesis of Methanol: Understanding the Requirements for an Industrial Catalyst for the Conversion of CO2. Angewandte Chemie - International Edition 55, 14906–14908. https://doi.org/10.1002/ANIE.201607600.

Borisut P, Nuchitprasittichai A. Process Configuration Studies of Methanol Production via Carbon Dioxide Hydrogenation: Process Simulation-Based Optimization Using Artificial Neural Networks. Energies 2020, Vol 13, Page 6608 2020;13:6608. 10.3390/EN13246608.

Borisut, P., Nuchitprasittichai, A., 2019. Methanol Production via CO2 Hydrogenation: Sensitivity Analysis and Simulation—Based Optimization. Front Energy Res 7, 81. https://doi.org/10.3389/FENRG.2019.00081/BIBTEX.

Borisut, P., Nuchitprasittichai, A., 2020. Optimization of methanol production via CO2 hydrogenation: comparison of sampling techniques for process modeling. IOP Conf Ser Mater Sci Eng 778 (1), 012088.

Bos, M.J., Kersten, S.R.A., Brilman, D.W.F., 2020. Wind power to methanol: Renewable methanol production using electricity, electrolysis of water and CO2 air capture. Appl Energy 264, 114672. https://doi.org/10.1016/J.APENERGY.2020.114672.

Bozzano, G., Manenti, F., 2016. Efficient methanol synthesis: Perspectives, technologies and optimization strategies. Prog Energy Combust Sci 56, 71–105. https://doi.org/10.1016/J.PECS.2016.06.001.

Bukhtiyarova, M., Lunkenbein, T., Kähler, K., Schlögl, R., 2017. Methanol Synthesis from Industrial CO2 Sources: A Contribution to Chemical Energy Conversion. Catal Letters 147, 416–427. https://doi.org/10.1007/S10562-016-1960-X.

Ari A, Arregui N, Black S, Celasun O, Iakova DM, Mineshima A, et al. Surging Energy Prices in Europe in the Aftermath of the War: How to Support the Vulnerable and Speed up the Transition Away from Fossil Fuels. 2022.

Cheng, F.Y., 1999. MULTIOBJECTIVE OPTIMUM DESIGN OF STRUCTURES WITH GENETIC ALGORITHM AND GAME THEORY: APPLICATION TO LIFE-CYCLE COST DESIGN. Computational Mechanics in Structural Engineering 1–16. https://doi.org/10.1016/B978-008043008-9/50039-9.

Dalena F, Senatore A, Marino A, Gordano A, Basile M, Basile A. Methanol Production and Applications: An Overview. Methanol: Science and Engineering 2018:3–28. 10.1016/B978-0-444-63903-5.00001-7.

Dimian, A.C., Bildea, C.S., Kiss, A.A., 2019. Methanol. Applications in Design and Simulation of Sustainable Chemical Processes 101–145. https://doi.org/10.1016/B978-0-444-63876-2.00003-6.

Din, I.U., Shaharun, M.S., Alotaibi, M.A., Alharthi, A.I., Naeem, A., 2019. Recent developments on heterogeneous catalytic CO2 reduction to methanol. Journal of CO2 Utilization 34, 20–33. https://doi.org/10.1016/J.JCOU.2019.05.036.

Eliseev K. District heating systems in Finland and Russia. 2011.

Emebu, S., Pecha, J., Janáčová, D., 2022. Review on anaerobic digestion models: Model classification & elaboration of process phenomena. Renewable and Sustainable Energy Reviews 160, 112288. https://doi.org/10.1016/J.RSER.2022.112288.

Erogbogbo, F., Lin, T., Tucciarone, P.M., LaJoie, K.M., Lai, L., Patki, G.D., Prasad, P.N., Swihart, M.T., 2013. On-demand hydrogen generation using nanosilicon: Splitting water without light, heat, or electricity. Nano Lett 13 (2), 451–456.

Etim, U.J., Song, Y., Zhong, Z., 2020. Improving the Cu/ZnO-Based Catalysts for Carbon Dioxide Hydrogenation to Methanol, and the Use of Methanol As a Renewable Energy Storage Media. Front Earth Sci (Lausanne) 8, 239. https://doi.org/10.3389/FENRG.2020.545431/BIBTEX.

European Environment Agency. Share of energy consumption from renewable sources in Europe 2022. https://www.eea.europa.eu/ims/share-of-energy-consumption-from (accessed December 27, 2022).

Finland Statistics, 2021. Energy in Finland 2021.

[27] Finnish Water Utilities Association. Finnish Industrial Wastewater Guide – conveying non-domestic wastewater to sewers . Helsinki : 2018.

Frost R. All the European countries returning to 'dirty' coal as Russia threatens to turn off the gas tap | Euronews 2022. https://www.euronews.com/green/2022/06/24/all-the-european-countries-returning-to-dirty-coal-as-russia-threatens-to-turn-off-the-gas (accessed December 27, 2022).

Ghosh, S., Sebastian, J., Olsson, L., Creaser, D., 2021. Experimental and kinetic modeling studies of methanol synthesis from CO2 hydrogenation using In2O3 catalyst. Chemical Engineering Journal 416, 129120. https://doi.org/10.1016/J.CEJ.2021.129120.

Gielen, D., Bazilian, M.D., 2021. Critically exploring the future of gaseous energy carriers. Energy Res. Soc Sci 79. https://doi.org/10.1016/j.erss.2021.102185.

Guil-López R, Mota N, Llorente J, Millán E, Pawelec B, Fierro JLG, et al. Methanol Synthesis from CO2: A Review of the Latest Developments in Heterogeneous Catalysis. Materials 2019, Vol 12, Page 3902 2019;12:3902. 10.3390/MA12233902.

Guil-López, R., Mota, N., Llorente, J., Millan, E., Pawelec, B.G., Fierro, J.L.G., et al., 2020. Unravelling the structural modification (Meso-nano-) of Cu/ZnO-Al2O3 catalysts for methanol synthesis by the residual NaNo3 in hydroxycarbonate precursors. Catalysts 10, 1–17. https://doi.org/10.3390/CATAL10111346.

Haldi, J., Whitcomb, D., 1967. Economies of Scale in Industrial Plants. Journal of Political Economy 75, 373–385. https://doi.org/10.1086/259293.

Holm-Larsen, H., 2001. CO2 reforming for large scale methanol plants - an actual case. Stud Surf Sci Catal 136, 441–446. https://doi.org/10.1016/S0167-2991(01)80343-8.

Hourng, L.W., Tsai, T.T., Lin, M.Y., 2017. The analysis of energy efficiency in water electrolysis under high temperature and high pressure. IOP Conf. Ser.: Earth Environ. Sci. 93, 012035.

Hunt, A.J., Sin, E.H.K., Marriott, R., Clark, J.H., 2010. Generation, Capture, and Utilization of Industrial Carbon Dioxide. ChemSusChem 3, 306–322. https://doi.org/10.1002/CSSC.200900169.

Ians, 2022. Germany increases coal power generation amid energy crisis. accessed December 27, 2022 Energy News, ET EnergyWorld. https://energy.economictimes.indiatimes.com/news/coal/germany-increases-coal-power-generation-amid-energy-crisis/94062809?redirect=1.

Idriss, H., 2020. Hydrogen production from water: past and present. Curr Opin Chem Eng 29, 74–82. https://doi.org/10.1016/J.COCHE.2020.05.009.

IEAGHG. CO2 capture at gas fired power plants. 2012.

Jeong, J.H., Kim, Y., Oh, S.Y., Park, M.J., Lee, W.B., 2022. Modeling of a methanol synthesis process to utilize CO2 in the exhaust gas from an engine plant. Korean Journal of Chemical Engineering 39, 1989–1998. https://doi.org/10.1007/S11814-022-1124-1/METRICS.

Jin, E., Zhang, Y., He, L., Harris, H.G., Teng, B., Fan, M., 2014. Indirect coal to liquid technologies. Appl Catal A Gen 476, 158–174. https://doi.org/10.1016/J.APCATA.2014.02.035.

Jung, J., Jeong, Y.S., Lim, Y., Lee, C.S., Han, C., 2013. Advanced CO2 capture process using MEA scrubbing: Configuration of a split flow and phase separation heat exchanger. Energy Procedia 37, 1778–1784. https://doi.org/10.1016/J.EGYPRO.2013.06.054.

Jurtz N. Automated workflow for spatially resolved fixed bed reactors with spherical and non-spherical particles 2014.

Kamsuwan, T., Krutpijit, C., Praserthdam, S., Phatanasri, S., Jongsomjit, B., Praserthdam, P., 2021. Comparative study on the effect of different copper loading

on catalytic behaviors and activity of Cu/ZnO/Al2O3 catalysts toward CO and CO2 hydrogenation. Heliyon 7 (7), e07682.
Kandasamy S, Manickam NK, Subbiah K, Muthukumar K, Kumaraguruparaswami M, Venkata Ratnam M. Nanotechnology's contribution to next-generation bioenergy production. Nanomaterials: Application in Biofuels and Bioenergy Production Systems 2021:511–8. 10.1016/B978-0-12-822401-4.00036-2.
Kanuri, S., Roy, S., Chakraborty, C., Datta, S.P., Singh, S.A., Dinda, S., 2022. An insight of CO2 hydrogenation to methanol synthesis: Thermodynamics, catalysts, operating parameters, and reaction mechanism. Int J Energy Res 46, 5503–5522. https://doi.org/10.1002/ER.7562.
Khor, C.S., Albahri, T.A., Elkamel, A., 2019. A model-based approach for optimizing petroleum refinery configuration for heavy oil processing. Computer Aided Chemical Engineering 46, 175–180. https://doi.org/10.1016/B978-0-12-818634-3.50030-8.
Klerk A. Transport Fuel: Biomass-, Coal-, Gas- and Waste-to-Liquids Processes. Future Energy: Improved, Sustainable and Clean Options for Our Planet 2020:199–226. 10.1016/B978-0-08-102886-5.00010-4.
Klier, K., 1982. Methanol Synthesis. Advances in Catalysis 31, 243–313. https://doi.org/10.1016/S0360-0564(08)60455-1.
Komu R, Hillberg S, Hovi V, Leppänen J, Leskinen J. A Finnish District Heating Reactor: Thermal-Hydraulic Design and Transient Analyses. International Conference on Nuclear Engineering, Proceedings, ICONE 2021;1. 10.1115/ICONE28-64163.
Kristensen, J.N., Christensen, P.L., Pedersen, K.S., Skovborg, P., 1993. A combined soave-redlich-kwong and NRTL equation for calculating the distribution of methanol between water and hydrocarbon phases. Fluid Phase Equilib 82, 199–206. https://doi.org/10.1016/0378-3812(93)87144-P.
Kuparinen, K., Vakkilainen, E., Tynjälä, T., 2019. Biomass-based carbon capture and utilization in kraft pulp mills. Mitig Adapt Strateg Glob Chang 24, 1213–1230. https://doi.org/10.1007/S11027-018-9833-9/TABLES/4.
Lemmens S. Cost Engineering Techniques and their Applicability for Cost Estimation of Organic Rankine Cycle Systems. Energies 2016, Vol 9, Page 485 2016;9:485. 10.3390/EN9070485.
Leonzio, G., 2018. State of art and perspectives about the production of methanol, dimethyl ether and syngas by carbon dioxide hydrogenation. Journal of CO2 Utilization 27, 326–354. https://doi.org/10.1016/J.JCOU.2018.08.005.
Liu, X.M., Lu, G.Q., Yan, Z.F., Beltramini, J., 2003. Recent Advances in Catalysts for Methanol Synthesis via Hydrogenation of CO and CO2. Ind Eng Chem Res 42, 6518–6530. https://doi.org/10.1021/IE020979S.
Lo, I.C., Wu, H.S., 2019. Methanol formation from carbon dioxide hydrogenation using Cu/ZnO/Al2O3 catalyst. J Taiwan Inst Chem Eng 98, 124–131. https://doi.org/10.1016/J.JTICE.2018.06.020.
Luyben, W.L., 2010. Design and Control of a Methanol Reactor/Column Process. Ind Eng Chem Res 49, 6150–6163. https://doi.org/10.1021/IE100323D.
Maeda, T., Nagata, Y., Endo, N., Ishida, M., 2016. Effect of water electrolysis temperature of hydrogen production system using direct coupling photovoltaic and water electrolyzer. Journal of International Council on Electrical Engineering 6, 78–83. https://doi.org/10.1080/22348972.2016.1173783.
Maxwell C. Cost Indices – Towering Skills 2022. https://www.toweringskills.com/financial-analysis/cost-indices/ (accessed December 27, 2022).
Mignard, D., 2014. Correlating the chemical engineering plant cost index with macro-economic indicators. Chemical Engineering Research and Design 92, 285–294. https://doi.org/10.1016/J.CHERD.2013.07.022.
Moioli, E., Schildhauer, T., 2022. Eco-Techno-Economic Analysis of Methanol Production from Biogas and Power-to-X. Ind Eng Chem Res 61, 7335–7348. https://doi.org/10.1021/ACS.IECR.1C04682/SUPPL_FILE/IE1C04682_SI_001.PDF.
Møller, K.T., Jensen, T.R., Akiba, E., Li, H., wen., 2017. Hydrogen - A sustainable energy carrier. Progress in Natural Science: Materials International 27, 34–40. https://doi.org/10.1016/J.PNSC.2016.12.014.
Nguyen, M.H., Prince, R.G.H., 1996. A simple rule for bioenergy conversion plant size optimisation: Bioethanol from sugar cane and sweet sorghum. Biomass Bioenergy 10, 361–365. https://doi.org/10.1016/0961-9534(96)00003-7.
Nguyen, T.B.H., Zondervan, E., 2019. Methanol production from captured CO2 using hydrogenation and reforming technologies_ environmental and economic evaluation. Journal of CO2 Utilization 34, 1–11. https://doi.org/10.1016/J.JCOU.2019.05.033.
Nieminen, H., Laari, A., Koiranen, T., 2019. CO2 hydrogenation to methanol by a liquid-phase process with alcoholic solvents: A techno-economic analysis. Processes 7 (7), 405.
Nyári J. Techno-economic feasibility study of a methanol plant using carbon dioxide and hydrogen. 2018.
Noriega, M.A., Narváez, P.C., 2020. Scale-up and cost analysis of biodiesel production using Liquid-Liquid Film Reactors: Reduction in the methanol consumption and investment cost. Energy 118724. https://doi.org/10.1016/j.energy.2020.118724.
Olabi, A.G., Wilberforce, T., Elsaid, K., Sayed, E.T., Maghrabie, H.M., Abdelkareem, M. A., 2022. Large scale application of carbon capture to process industries – A review. J Clean Prod 362, 132300. https://doi.org/10.1016/J.JCLEPRO.2022.132300.
Peng, X.D., Toseland, B.A., Underwood, R.P., 1997. A novel mechanism of catalyst deactivation in liquid phase synthesis Gas-to-DME reactions. Stud Surf Sci Catal 111, 175–182. https://doi.org/10.1016/S0167-2991(97)80153-X.
Pérez-Fortes, M., Schöneberger, J.C., Boulamanti, A., Tzimas, E., 2016. Methanol synthesis using captured CO2 as raw material: Techno-economic and environmental assessment. Appl Energy 161, 718–732. https://doi.org/10.1016/J.APENERGY.2015.07.067.
Porosoff, M.D., Yan, B., Chen, J.G., 2016. Catalytic reduction of CO2 by H2 for synthesis of CO, methanol and hydrocarbons: challenges and opportunities. Energy Environ Sci 9, 62–73. https://doi.org/10.1039/C5EE02657A.
Portha, J.-F., Parkhomenko, K., Kobl, K., Roger, A.-C., Arab, S., Commenge, J.-M., Falk, L., 2017. Kinetics of Methanol Synthesis from Carbon Dioxide Hydrogenation over Copper-Zinc Oxide Catalysts. Ind Eng Chem Res 56 (45), 13133–13145.
Puentes, C., Joulia, X., Athès, V., Esteban-Decloux, M., 2018. Review and Thermodynamic Modeling with NRTL Model of Vapor-Liquid Equilibria (VLE) of Aroma Compounds Highly Diluted in Ethanol-Water Mixtures at 101.3 kPa. Ind Eng Chem Res 57, 3443–3470. https://doi.org/10.1021/ACS.IECR.7B03857.
Rakić, T., Kasagić-Vujanović, I., Jovanović, M., Jančić-Stojanović, B., Ivanović, D., 2014. Comparison of Full Factorial Design, Central Composite Design, and Box-Behnken Design in Chromatographic Method Development for the Determination of Fluconazole and Its Impurities. Http://DxDoiOrg/101080/000327192013867503 47, 1334–1347. https://doi.org/10.1080/00032719.2013.867503.
Remer, D.S., Chai, L.H., 1993. Process Equipment, Cost Scale-up vol. 43, 306–317.
Turton Richard, Shaeiwitz Joseph A., Bhattacharyya Debangsu, Whiting Wallace B. Analysis, Synthesis and Design of Chemical Processes. Pearson; 2018.
Rosha, P., Kumar, S., Ibrahim, H., 2021. A thermodynamic analysis of biogas-to-methanol conversion with CH4 recycling and CO2 utilization using Aspen HYSYS. Sustain Energy Fuels 5, 4336–4345. https://doi.org/10.1039/D1SE00514F.
Saarinen, T., Vuori, K.M., Alasaarela, E., Kløve, B., 2010. Long-term trends and variation of acidity, CODMn and colour in coastal rivers of Western Finland in relation to climate and hydrology. Science of the Total Environment 408, 5019–5027. https://doi.org/10.1016/J.SCITOTENV.2010.07.009.
Saeidi, S., Amin, N.A.S., Rahimpour, M.R., 2014. Hydrogenation of CO2 to value-added products—A review and potential future developments. Journal of CO2 Utilization 5, 66–81. https://doi.org/10.1016/J.JCOU.2013.12.005.
Saito, M., Fujitani, T., Takahara, I., Watanabe, T., Takeuchi, M., Kanai, Y., Moriya, K., Kakumoto, T., 1995. Development of Cu/ZnO-based high performance catalysts for methanol synthesis by CO2 hydrogenation. Energy Convers Manag 36 (6-9), 577–580.
Samiee L, GhasemiKafrudi E. Assessment of different kinetic models of carbon dioxide transformation to methanol via hydrogenation, over a Cu/ZnO/Al2O3 catalyst. Reaction Kinetics, Mechanisms and Catalysis 2045;133:801–23. 10.1007/s11144-021-02045-1.
Sarp, S., Gonzalez Hernandez, S., Chen, C., Sheehan, S.W., 2021. Alcohol Production from Carbon Dioxide: Methanol as a Fuel and Chemical Feedstock. Joule 5, 59–76. https://doi.org/10.1016/J.JOULE.2020.11.005.
Schorn, F., Breuer, J.L., Samsun, R.C., Schnorbus, T., Heuser, B., Peters, R., Stolten, D., 2021. Methanol as a renewable energy carrier: An assessment of production and transportation costs for selected global locations. Advances in Applied Energy 3, 100050.
Siqueira, R.M., Freitas, G.R., Peixoto, H.R., Nascimento, J.F.d., Musse, A.P.S., Torres, A. E.B., Azevedo, D.C.S., Bastos-Neto, M., 2017. Carbon Dioxide Capture by Pressure Swing Adsorption. Energy Procedia 114, 2182–2192.
Song, H., Luo, S., Huang, H., Deng, B., Ye, J., 2022. Solar-Driven Hydrogen Production: Recent Advances, Challenges, and Future Perspectives. ACS Energy Lett 7, 1043–1065. https://doi.org/10.1021/ACSENERGYLETT.1C02591/ASSET/IMAGES/LARGE/NZ1C02591_0009.JPEG.
Stoica, I., Banu, I., Bobarnac, I., Bozga, G., 2015. Optimization of a methanol synthesis reactor. Series B, Bull, p. 77.
Stokes CA, Stokes HC. The economics of methanol production in nigeria based on large low-cost gas resources. 2002.
Tanttu, U., Jokela, P., 2018. Sustainable drinking water quality improvement by managed aquifer recharge in Tuusula region. Finland. Sustain Water Resour Manag 4, 225–235. https://doi.org/10.1007/S40899-017-0198-0.
Tao, M., Li, J., Theodoropoulos, C., 2019. Reduced model-based global optimisation of large-scale steady state nonlinear systems. Computer Aided Chemical Engineering 46, 1039–1044. https://doi.org/10.1016/B978-0-12-818634-3.50174-0.
Taylor K. LEAK: Energy prices will 'remain high and volatile until at least 2023', EU Commission says – EURACTIV.com 2022. https://www.euractiv.com/section/energy/news/leak-energy-prices-will-remain-high-and-volatile-until-at-least-2023-eu-commission-says/ (accessed December 27, 2022).
Tosun, I., 2013. Calculation of Changes in Internal Energy, Enthalpy, and Entropy. The Thermodynamics of Phase and Reaction Equilibria 35–104. https://doi.org/10.1016/B978-0-44-459497-6.00003-7.
Ulrich, G.D., Vasudevan, P.T., 2006. How to Estimate Utility Costs.
Updating, V.WM., 2002. the Plant Cost Index.
Vamvuka, D., 2011. Bio-oil, solid and gaseous biofuels from biomass pyrolysis processes—An overview. Int J Energy Res 35, 835–862. https://doi.org/10.1002/ER.1804.
Van-Dal, É.S., Bouallou, C., 2013. Design and simulation of a methanol production plant from CO2 hydrogenation. J Clean Prod 57, 38–45. https://doi.org/10.1016/J.JCLEPRO.2013.06.008.
Vetere, A., 2004. The NRTL equation as a predictive tool for vapor-liquid equilibria. Fluid Phase Equilib 218, 33–39. https://doi.org/10.1016/J.FLUID.2003.10.013.
Wang, H., Chen, J., Li, Q., 2019. A Review of Pipeline Transportation Technology of Carbon Dioxide. IOP Conf. Ser.: Earth Environ. Sci. 310 (3), 032033.
Wang Y, Chang M, Chen L, Wang S, Fan S, Hua D. Evaluation of Prediction Models for the Physical Properties in Fire-Flooding Exhaust Reinjection Process. Energies 2022, Vol 15, Page 562 2022;15:562. 10.3390/EN15020562.
Wang, X., Song, C., 2020. Carbon Capture From Flue Gas and the Atmosphere: A Perspective. Front Energy Res 8, 265. https://doi.org/10.3389/FENRG.2020.560849/BIBTEX.
Warudkar, S.S., Cox, K.R., Wong, M.S., Hirasaki, G.J., 2013. Influence of stripper operating parameters on the performance of amine absorption systems for post-combustion carbon capture: Part II. Vacuum strippers. International Journal of

Greenhouse Gas Control 16, 351–360. https://doi.org/10.1016/J.IJGGC.2013.01.049.
West, A.H., Posarac, D., Ellis, N., 2008. Assessment of four biodiesel production processes using HYSYS.Plant. Bioresour Technol 99, 6587–6601. https://doi.org/10.1016/J.BIORTECH.2007.11.046.
Yusuf, N., Almomani, F., 2023. Highly effective hydrogenation of CO2 to methanol over Cu/ZnO/Al2O3 catalyst: A process economy & environmental aspects. Fuel 332, 126027. https://doi.org/10.1016/J.FUEL.2022.126027.
Zang, G., Sun, P., Elgowainy, A., Wang, M., 2021. Technoeconomic and Life Cycle Analysis of Synthetic Methanol Production from Hydrogen and Industrial Byproduct CO2. Environ Sci Technol 55, 5248–5257. https://doi.org/10.1021/ACS.EST.0C08237/SUPPL_FILE/ES0C08237_SI_001.PDF.
Zhang, F., Xu, X., Qiu, Z., Feng, B.o., Liu, Y., Xing, A., Fan, M., 2022. Improved methanol synthesis performance of Cu/ZnO/Al2O3 catalyst by controlling its precursor structure. Green Energy and Environment 7 (4), 772–781.
Zhong, J., Yang, X., Wu, Z., Liang, B., Huang, Y., Zhang, T., 2020. State of the art and perspectives in heterogeneous catalysis of CO2 hydrogenation to methanol. Chem Soc Rev 49, 1385–1413. https://doi.org/10.1039/C9CS00614A.
Zohuri, B., 2018. Properties of Pure Substances. Physics of Cryogenics 53–79. https://doi.org/10.1016/B978-0-12-814519-7.00002-1.